

Ultrafast electron diffraction

Xuan Wang(王瑄), Yutong Li(李玉同)

Citation: Chin. Phys. B . 2018, 27(7): 076102. **doi:** 10.1088/1674-1056/27/7/076102

Journal homepage: http://cpb.iphy.ac.cn; http://iopscience.iop.org/cpb

What follows is a list of articles you may be interested in

Superconductivity in electron-doped arsenene

Xin Kong(孔鑫), Miao Gao(高淼), Xun-Wang Yan(闫循旺), Zhong-Yi Lu(卢仲毅), Tao Xiang(向涛)

Chin. Phys. B . 2018, 27(4): 046301. **doi:** 10.1088/1674-1056/27/4/046301

Theoretical description of electron-phonon Fock space for gapless and gapped nanowires

Ashrafalsadat Shariati, Hassan Rabani, Mohammad Mardaani

Chin. Phys. B . 2017, 26(3): 036302. **doi:** 10.1088/1674-1056/26/3/036302

Two-coupled structural modulations in charge-density-wave state of $SrPt_2As_2$ superconductor

Wang Li, Wang Zhen, Shi Hong-Long, Chen Zhen, Chiang Fu-Kuo, Tian Huan-Fang, Yang Huai-Xin, Fang Ai-Fang, Wang Nan-Lin, Li Jian-Qi

Chin. Phys. B . 2014, 23(8): 086103. **doi:** 10.1088/1674-1056/23/8/086103

Periodic, quasiperiodic, and chaotic breathers in two-dimensional discrete β-Fermi-Pasta-Ulam lattice

Xu Quan, Tian Qiang

Chin. Phys. B . 2013, 22(8): 086302. **doi:** 10.1088/1674-1056/22/8/086302

TOPICAL REVIEW — Synergetic Extreme Condition User Facility: Breakthroughs and opportunities for the research of physical science

Ultrafast electron diffraction*

Xuan Wang(王瑄)[1,†] and Yutong Li(李玉同)[1,2,3,‡]

[1] *Beijing National Laboratory for Condensed Matter Physics, Institute of Physics, Chinese Academy of Sciences, Beijing* 100190, *China*
[2] *School of Physical Sciences, University of Chinese Academy of Sciences, Beijing* 100049, *China*
[3] *Collaborative Innovation Center of IFSA (CICIFSA), Shanghai Jiao Tong University, Shanghai* 200240, *China*

(Received 21 March 2018; revised manuscript received 19 May 2018; published online 1 June 2018)

Ultrafast electron diffraction (UED) technique has proven to be an innovative tool for providing new insights in lattice dynamics with unprecedented temporal and spatial sensitivities. In this article, we give a brief introduction of this technique using the proposed UED station in the Synergetic Extreme Condition User Facility (SECUF) as a prototype. We briefly discussed UED's functionality, working principle, design consideration, and main components. We also briefly reviewed several pioneer works with UED to study structure-function correlations in several research areas. With these efforts, we endeavor to raise the awareness of this tool among those researchers, who may not yet have realized the emerging opportunities offered by this technique.

Keywords: ultrafast phenomena, lattice dynamics, ultrafast electron diffraction

PACS: 63.20.kd, 63.20.Ry, 63.90.+t, 61.05.J– **DOI:** 10.1088/1674-1056/27/7/076102

1. Introduction

Structural dynamics is of great importance in science and technology, as it governs many fundamental processes in nature, such as phase transitions, chemical reactions, and biological functions. It is also correlated to other dynamical responses of materials involving electronic, magnetic, and other degrees of freedom, which account for most of materials' functionalities.[1] A through understanding of structural dynamics and its complex correlation to other degrees of freedom requires synergetic use of multiple techniques to provide complementary views. Ultrafast electron diffraction (UED) technique addresses such request by providing real-time and atomic-level view of structural dynamics. Thanks to a number of parallel revolutionary advances in ultrafast laser technology, and in generation and control of ultrafast electron probes, UED now reaches a temporal resolution of 100 femtoseconds (fs) that is only multiples of the vibrational period of atoms, and a spacial sensitivity of 0.01 Å that is only a fraction of inter-atomic distance. The combination of such atomic-level temporal and spacial details holds the potential to fully reveal the physical mechanisms and the structure-function correlations that would otherwise be impossible to extract.

In this article, we briefly discussed UED technique by introducing the architecture of the proposed UED station in the Synergetic Extreme Condition User Facility (SECUF). We discussed what information can be obtained by UED and its comparison with ultrafast x-ray. With this foundation, we gave a very brief review of several pioneering works with UED that provide new insights into chemical reactions, electron–phonon coupling, structural phase transitions, and so on. In overall, the aim of this review is to attract potential users for this new user facility and encourage new strategies to take full advantage of various tools in SECUF to tackle complex multi-discipline problems.

2. Electron as a ultrafast probe

2.1. Diffraction

Diffraction refers to the phenomena that a wave deviates from its original propagating direction due to interference caused by obstacles, apertures, and so on. It is mostly pronounced when the wavelength is comparable to the dimension of the scattering elements. Particularly, electron diffraction has been widely used for material characterization, in which electrons are usually accelerated to very high energy (1 keV to 100 keV) so that their de Broglie wavelengths become a few percent of typical inter-atomic distance ensuring the resolution of atomic-level details.

For elastic scattering and by considering the superpositions of the reflections from adjacent parallel lattice planes (see Fig. 1), the criterion of constructive interference (or formation of diffraction peaks) is described by Bragg's law[2]

$$2d_{(h,k,l)}\sin(\theta) = \lambda, \tag{1}$$

*Project supported by the National Natural Science Foundation of China (Grant No. 11774409), the National Basic Research Program of China (Grant No. 2013CBA01501), and the Strategic Priority Research Program of the Chinese Academy of Sciences (Grant Nos. XDB16010200 and XDB07030300).

†Corresponding author. E-mail: xw@iphy.ac.cn
‡Corresponding author. E-mail: ytli@iphy.ac.cn

© 2018 Chinese Physical Society and IOP Publishing Ltd

where $d_{(h,k,l)}$ is the distance between adjacent parallel planes indexed by Miller indices (h,k,l), θ is the reflection angle, and λ is the de Broglie wavelength of electrons. Since each family of parrel planes (h,k,l) corresponds to a vector $\boldsymbol{g}_{(h,k,l)}$ in reciprocal lattice space, the equivalent diffraction law in the reciprocal space can be written as

$$\boldsymbol{k}' - \boldsymbol{k} = \boldsymbol{g}, \tag{2}$$

where $\boldsymbol{k}$ and $\boldsymbol{k}'$ are the wave vectors of the original and the diffracted beams, whose magnitudes are defined as $k = k' = 2\pi/\lambda$. This represents Laue conditions for constructive interference and is more convenient to use for indexing diffraction spots.

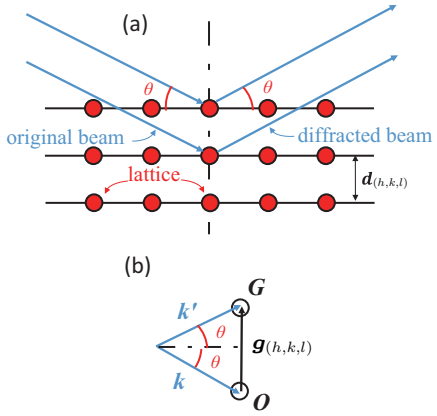


Fig. 1. (color online) (a) Bragg diffraction in real space. Two beams with identical wavelength and phase approach a crystalline solid and are scattered off two parallel planes of atoms. The lower beam traverses an extra length. Constructive interference occurs when this length is equal to an integer multiple of the wavelength of the radiation. (b) Laue condition in reciprocal space. Constructive interference occurs when the difference between the wave vectors of the original and the diffracted beams equals to a reciprocal vector.

Bragg's law or Laue formulation only tells (yet awarded two Nobel Prizes) where the centers of diffraction peaks locate. To fully comprehend the spacial intensity distribution in a diffraction pattern, kinematical theory, or more advanced theories, such as dynamical theory or quantum mechanical treatment, must be used depending on experimental conditions.[2] Inelastic or diffusive scattering may also be considered under certain conditions. With these efforts, rich information of samples including lattice temperature, lattice strain, grain orientation, and so on can be extracted. Also, the equivalence between real space and reciprocal space enables the construction of complex structures, e.g., biomolecules, when direct imaging is impractical.[3]

Diffraction has its unique advantages in resolving structural dynamics, because it is very sensitive to internuclear coordinates (correlation between the positions of atoms) as implied by Bragg's law. Bond lengths, bond angles, and lattice constants are examples of the measures in such coordinates, which are more relevant to "changes" in a structure. In a typical UED experiment, only limited number of internuclear coordinates are altered by laser excitation, while the others are treated as statical background. This is an important difference of data analysis between UED and transmission electron microscopy (TEM), and in most cases, makes the data analysis of UED much simplified.

2.2. Advantage and disadvantage in using electrons

Diffraction provides a direct measure of the structural information with unprecedented spacial sensitivity. When coupled with time resolution, ultrafast diffraction yields a "real-time" probe of structural dynamics. Both x-rays and electrons can serve as probes for ultrafast diffraction, and they are complementary to each other.[4,5] The advantage of using electrons underlies in their strong Coulomb interaction with most samples. The elastic scattering cross-section for electrons (80 keV to 500 keV) is 10^5 to 10^6 in magnitude of that of x-rays,[6] such that the elastic scattering length (10 nm to 100 nm) of electrons better matches the optical penetration depth of the pump laser pulses. This means much stronger dynamical signals and more homogeneous excitation for thin samples in UED. Meanwhile, electrons can be more easily accelerated and collimated (focused or deflected) with well-developed electron-optics for very high spacial resolution. The beam size of electron probes can be controlled to even nanometer scale for nano-diffraction to reveal local structural feature, while its counterpart x-ray would not be able to deliver. The energy deposited by inelastic scattering event per elastic scattering event for electrons (80 keV to 500 keV) is three orders less in magnitude than x-ray (0.15 nm in wavelength).[6] So electrons are less damaging if the same amount of signals (elastic scattering events) are collected.

Turning to the other side of the coin, strong Coulomb interaction also brings many challenges for UED. The first issue is the sample preparation. In most cases, the thickness of a pristine sample needs to be reduced to less than 100 nm like in TEM. But the requirement for UED is even higher, for the typical transverse beam size of the electron probe in UED is in the order of 100 μm, much larger than that in TEM. Since electrons are so sensitive to electromagnetic field, transient electric or magnetic field can deviate electron's trajectory, introducing artifacts into diffraction patterns.[7–9] Besides, space-charge effect (the repulsive force among electrons within each electron bunch) tends to broaden its longitudinal duration. For example, an electron bunch containing only few thousand 100 keV electrons broadens from several tenth fs at birth to more than one picosecond (ps) only after propagating about half meter long.[10,11] This is the key factor that degrades the temporal resolution of UED, because it relies on very short (longitudinally) electron bunch to "freeze" a transient moment

of a dynamical process, just like each frame in a video.

Space-charge effect not only motivates many theoretical works to model electron-bunch propagation[10,12–14] but also leads to several important developing directions of UED technique. Reviewing the history of UED, the early apparatus are always very compact cutting down the time interval between the birth of electrons and their arrival at sample's location as much as possible.[15–17] Meanwhile, the number of electrons per bunch is reduced to about 10^3 to 10^4. The combination of short propagation time and low fluence enables UED to achieve sub-ps temporal resolution.[18,19] To obtain even better temporal resolution, or in the case when the transverse beam dimension is focused tightly, such as in ultrafast converge beam diffraction (UCBD)[20] or ultrafast electron microscopy (UEM),[21,22] the number of electrons per bunch is reduced to even less than ten. Another strategy is to utilize a streaking camera to obtain temporal resolution, and therefore partially loosen the requirement of very short bunch duration.[23] It is more desirable if the contradiction between high fluence and high temporal resolution can be resolved, and recently two new schemes are introduced to tackle this issue. The first one is MeV electron diffraction technique (MeV UED), in which electrons are accelerated to MeV and the relativistic effect slows down the bunch expansion in the lab frame.[24–31] Remarkably, more than 10^6 electrons can be packed in a bunch while keeping a longitudinal duration in the order of 100 fs. The second scheme is to leave the space-charge broadening initially, and then compress the bunch duration all the way to sub-ps range right at its arrival at sample's location.[32–34] In this case, 10^5 to 10^6 electrons per pulse are achieved with sub-ps longitudinal duration, or very few electrons are bunched for even shorter duration (fs scale).[35] In this paper, we will focus on the second scheme, which is applied for the UED station in SECUF.

3. Experimental set-up and design consideration

3.1. Figures of merit

Critical considerations for UED experiments are the mechanism used to initiate dynamics, spacial sensitivity, temporal resolution, electron fluence, and coherent length for diffraction. Ultrafast laser can provide various stimulus to the material, such as ultrafast heating, coherent phonon generation, bond alteration, and so on. Since the laser pulse is very short, it also determines the time-zero of the stimulated dynamical process.

The relevant spacial sensitivity for UED should be a fraction of the quantities measured in internuclear coordinates, e.g., bond lengths or lattice constants. We want to emphasize that spacial sensitivity of UED is different from spacial resolution used for imaging. As mentioned in previous section, UED is sensitive to internuclear coordinates, and spacial sensitivity characterizes how much change in such coordinates that UED can resolve, for example, how much lattice constants change after certain stimulus. It does not mean that UED can image an atom nor can it pin down atom's exact position with such high spacial resolution. In fact, the transverse beam size of UED is so large (100 μm) that a big amount of atoms in the probed area contribute to diffraction signals to achieve such high spacial sensitivity. Nevertheless, as we will show later, abundant information regarding transient lattice dynamics has been obtained from snapshots of diffraction patterns in absence of high-resolution images.

The relevant temporal resolution for lattice dynamics is a single vibrational period that varies from sample to sample. For example, the fastest atomic vibration period is around 10 fs involving light elements such as O–H bond and C–H bond,[5,36] and the corresponding length scale of such vibration is only in the order of 0.01 Å. If bond breaking is studied, the relent time scale extends to more than 100 fs, because it involves much larger change in the length of the bond. Such time-scale is also valid for lattice dynamics in solids, because the periods of optical phonon modes are usually several hundred fs. It can be achieved nowadays by a typical UED set-up and new techniques are aiming for sub-fs temporal resolution.[37]

Electron-bunch duration is not the only factor that determines the temporal resolution of UED. Assuming all contributing factors are independent to one another, the overall temporal resolution can be estimated by

$$\tau_{\text{total}} = (\tau_{\text{pump}}^2 + \tau_{\text{probe}}^2 + \tau_{\text{mis}}^2 + \tau_{\text{jitter}}^2)^{1/2}, \tag{3}$$

where τ_{pump} and τ_{probe} are the longitudinal durations of the pump and probe, respectively, and τ_{jitter} is the timing jitter between them, which will be elaborated later. τ_{mis} is the temporal smearing introduced by their different velocities and geometric arrangements (see Fig. 2). For transmission geometry, τ_{mis} can be estimated by

$$\tau_{\text{mis}} \approx d_{\text{s}}/v_{\text{e}} - d_{\text{s}}\cos(\alpha)/c + l_{\text{e}}\sin(\alpha)/c, \tag{4}$$

where v_{e} and c are the velocities of electrons and photons, respectively. For 100 keV electrons and $\alpha < 10^{\circ}$, $\tau_{\text{mis}} < 100$ fs for a typical thin film. However, it increases to the order of ps for gas phase, whose effective thickness in an experiment is several hundred μm. For reflection geometry, τ_{mis} can be estimated by

$$\tau_{\text{mis}} \approx l_{\text{e}}/(v_{\text{e}}\sin(\alpha)). \tag{5}$$

Since the glancing angle α is only several degrees, τ_{mis} is tenth of ps. Pulse-tilting scheme is ultilized to reduce τ_{mis} to the order of 100 fs for gas phase and reflection geometry.[38,39]

The electron fluence is defined as N_{e}/A, where N_{e} is the number of electrons per bunch and A is the transverse area of

the electron beam. It must fit to the degree of the reversibility of the investigated processes, e.g., a fluence more than 10^8 cm^{-2} is required to study irreversible process.[4,5] For reversible processes, the electron fluence can be largely reduced depending on the repetition rate of the laser system.

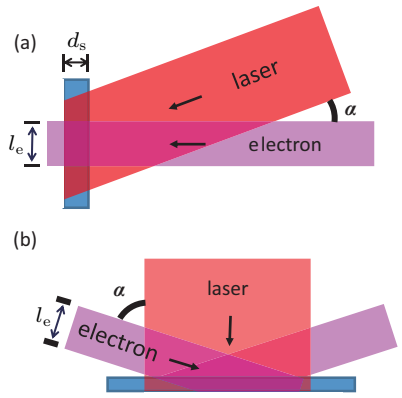


Fig. 2. (color online) (a) Transmission and (b) reflection set-up for a typical UED experiment.

The required coherent length for diffraction depends on the unit cell of materials. For small molecules or solid-state lattice, the unit cell is usually smaller than 1 nm, and it can be handled by a typical UED's electron probe whose coherent length is usually several nm.[5] However, for biomolecular samples, the unit cell can reach 10 nm, which becomes a challenge for UED. New electron probes from ultracold sources[40] or nano-scale tips[41] are under development to tackle this issue.

The figures of merit of UED station in SECUF are listed in Table 1.

Table 1. Figures of merit.

Parameter	Value
Spacial sensitivity	$\lesssim 0.01$ Å
Temporal resolution	$\lesssim 500$ fs
Electron fluence	$\gtrsim 10^9$ cm^{-2}
Transverse beam size	~ 100 μm
Coherent length	$\gtrsim 2$ nm

3.2. Experimental set-up

In SECUF, we are proposed to build a new UED station based on the pulse compression scheme. As shown in Fig. 3, the new station consists of an ultrafast laser, an ultrafast electron gun, a collimation and compression unit, a sample preparation unit, a ultra-high vacuum (UHV) target chamber, and a detection unit. During the experiment, short laser pulses centered at 800 nm are generated by the ultrafast laser system and split into two arms. One is sent to an optical parametric amplification (OPA) system to change the wavelength, and guided to the sample as the pump beam. The other one, whose frequency is tripled by an optical tripler, is guided to the photocathode of the ultrafast electron gun to generate short electron pulses as the probe beam. These electron pulses are collimated (deflected or focused) during their propagation. They are then guided into a pulse compressor, where an inverse electric field is generated by a radio-frequency cavity to flip the electron velocity distribution (see later context for details). As a result, the pulse duration starts to reduce gradually to a minimum at the position where the sample is located (see the sketch of how the bunch duration evolves in Fig. 3). Interacting with the sample, electrons form diffraction patterns, which are recorded by the detection unit. This is a typical pump–probe method, where the relative time interval between the pump and probe is controlled by a motion stage.

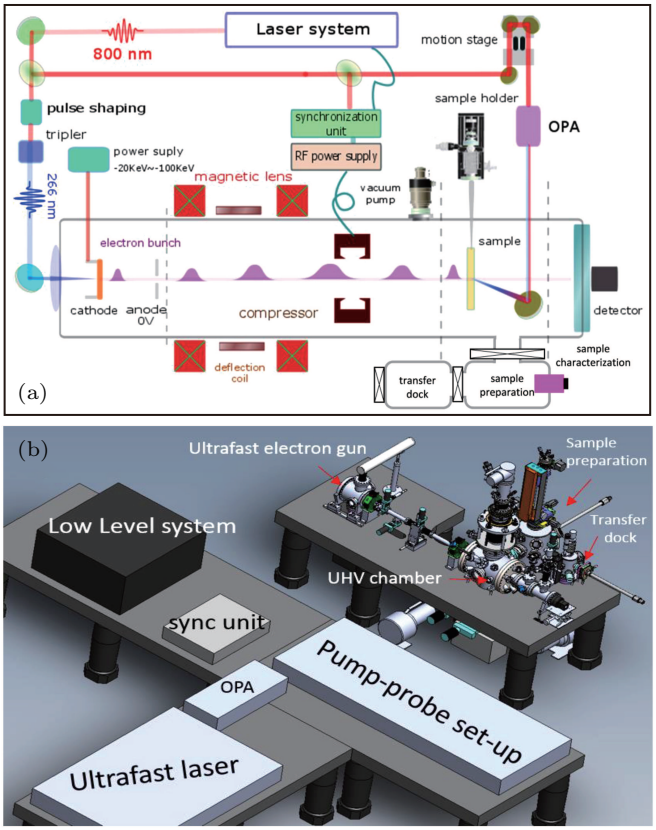


Fig. 3. (color online) (a) Schematic diagram of the experimental set-up shows the main components and (b) 3D effect drawing of the whole system under construction.

3.2.1. Ultrafast laser

The ultrafast laser system is a typical CPA system that produces short laser pulses with 60 fs pulse duration centered at 800 nm and 7 mJ maximal pulse energy at 1 kHz repetition rate. The optical cavity of the oscillator can be tuned in order to synchronize with a radio frequency clock (3 GHz). The laser system provides seeds for both pump and probe. The pump seed is sent to an OPA to change wavelength (20 μm to 240 nm) depending on materials under investigation. The intensity profile of the probe seed will be first optimized to a cylindrical bear-can shape (transversely top-hat and longitudinally square), and then the pulse will be frequency tripled

(corresponding to 266 nm in wavelength) in order to exceed the work function of the metal photocathode.

3.2.2. Ultrafast electron gun

The ultrafast electron gun consists of a photocathode and an anode separated by about 8 mm, producing an acceleration field of more than 10^5 V/cm when operating at 100 keV. For lower electron energy, the gap will be narrowed to maintain the same acceleration field. The photocathode is made of metal (silver or copper) coated on a fused silica disk, which can generate photoelectrons under the excitation of 266 nm laser pulses. The initial energy spread of electrons is regulated to below 0.5 eV in order to achieve a transverse coherent length of several nm. The applied acceleration field is much larger than the image-charge field induced by the electron bunches near the photocathode, ensuring the intensity profile of the electron bunches resembling the laser seeds. Such profile prevents the emittance growth from the space-charge effect, and therefore leads to a better coherent length. However, to maintain such a high field, careful design, fine machining, and a systematic conditioning procedure must be applied to the e-gun in order to avoid high voltage break-down.

3.2.3. Collimation and compression unit

This is the key unit for obtaining sub-ps electron bunches with high electron fluence. The transverse dimension and the trajectory of electron bunches are controlled by magnetic lens and deflection coil, respectively, similar as in a typical TEM, while the pulse duration is controlled by the pulse compressor. So, the system achieves three-dimensional control of the density profile of the electron bunches. The principle for pulse compression is shown in Fig. 4(a) (also see the evolution of the electron-bunch duration in Fig. 3(a)). After the electron propagates for several nanoseconds, the longitudinal density profile of the electron bunch in its phase-space is linearly chirped so that faster electrons move to the head leaving the slower ones at the tail. When entering the compressor, a transient electric field is applied with a frequency of about 3 GHz. Since the pulse duration is around 10 ps at this moment, the transient field can be considered linear in time, which inverses the linear velocity chirp of the electron bunch in the phase-space. After the inversion, electrons in head and tail will move towards the center of the bunch so that its duration gradually shrinks to a minimum, and then expands again. Considering the compressor as a longitudinal lens, our sample will be put on its focus for the best temporal resolution. The predicted achievable pulse duration by compression is smaller than 10 fs, but experimental results are in the order of 100 fs for 1 million electrons per pulse. Several factors may prevent further compression including inhomogeneous space-charge effect, non linearity in the compression field, the edge field in the RF compressor, and so on. Another critical issue for this compression scheme is the synchronization between one electron bunch and the compression field. Ideally, the center of the electron bunch should arrive at the center of the cavity when the magnitude of the compression field is zero as shown in Fig. 4(b). Timing mismatch between the two will lead to either an increase or decrease of the group velocity of the electron bunch, which leads to an advance or delay of its arrival at sample's location. However, the timing of the pump beam is not affected by this timing change, and therefore an additional uncertainty τ_{jitter} is introduced which impairs the overall temporal resolution as indicated in Eq. (5). In our system, a comprehensive synchronization scheme is developed to obtain $\tau_{\text{jitter}} \approx 100$ fs.

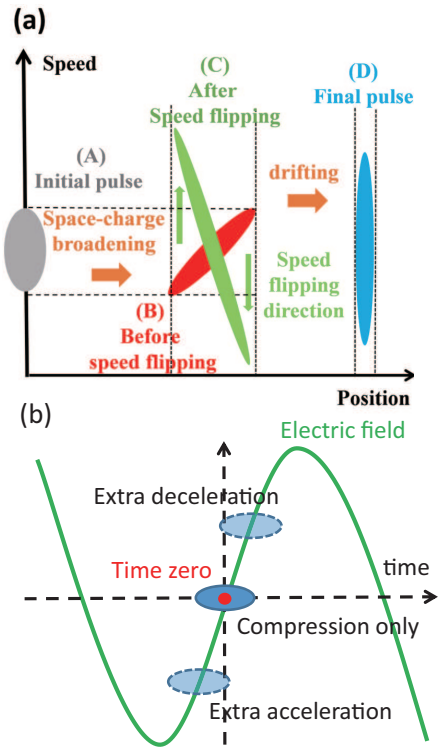


Fig. 4. (color online) (a) Longitudinal phase space diagram for an electron bunch during its propagation. (A) The initial velocity distribution (shown in grey). (B) A velocity chirp is built-up in phase space (shown in red) due to space charge effect. (C) Distribution of velocity is flipped (shown in green) such that the bunch starts to compress. (D) The bunch reduces to its minimal duration (shown in blue). (b) Relative timing between the electron bunch and the transient electric field from the compressor, which can cause timing jitter if it changes randomly.

3.2.4. Sample preparation unit

This unit is mainly composed of an ion sputter gun, low energy electron diffracion (LEED) with Auger electron spectroscope (AES), evaporation sources, a continuous electron source, and a heating-cooling sample holder, all of which are operating under UHV. It is fully equipped for surface science, and for photocathode fabrication. Also, before each time-resolved experiment, statical diffraction patterns are first taken by the continuous electron probe to evaluate the quality of the sample.

3.2.5. UHV target chamber

This unit contains a multi-functional sample holder that is suitable for both transmission and reflection diffraction experiments. Sample's temperature can be adjusted from 10 K to 1000 K. Other accessories include a Faraday cup to measure the number of electrons per pulse, a streaking module to measure the electron pulse duration, several guiding mirrors for the pump laser, several view ports for beam alignment, and a differential pumping system for gas dosing. The design of the whole unit is optimized for surface science, which is one advantage of our instrument if comparing with other UED apparatus.

3.2.6. Detection unit

The diffracted electrons are first converted into photons by a fast-decay (0.11 μs) P47 phoshor screen coated by 100 nm aluminum foil in front to block the scattering light from the pump. Then they are recorded by a CCD camera. If the intensity of the signal is weak, an image intensifier will be inserted in front of the camera to gain an extra 10^5 amplification, which is very useful for a time-resolved reflective high energy electron diffraction (RHEED) or a single-shot experiment.

4. Applications

Since its unique ability in monitoring structural dynamics, UED has been developing rapidly, and now dozens of UED apparatus are established or under construction worldwide. The research topics are also expanding fast including gas phase, surface science, strong correlated system, nanostructre, and so on. In this section, we do not intend to review all these aspects but rather pick several topics to demonstrate the ability of UED technique.

4.1. Gas phase studies

Using electron diffraction to study statical structures of gas molecules can date back to 1930, only three years after its invention. Despite angular averaging over randomly-distributed molecular orientations and lack of long-range orders, the accuracy of modern gas-phase electron diffraction can approach 10^{-4} Å,[4] thanks to the large scattering cross section of electrons and the advance in data analysis methods. The total scattering intensity can be written as $I = I_{\rm A}(s) + I_{\rm M}(s)$, where $I_{\rm A}$ is the atomic scattering intensity expressed as an algebraic summation of the contribution from each individual atom. $I_{\rm M}$ is the interfering term from each atom–atom pair, which can be written as

$$I_{\rm M}(s) = C\sum_{i=1}^{N}\sum_{j-i}^{N} |f_i||f_j| \exp\left(-\frac{1}{2}l_{ij}^2 s^2\right) \times \cos(\eta_i - \eta_j)\frac{\sin(sr_{ij})}{sr_{ij}}, \quad (6)$$

where f_i is the elastic scattering amplitude for the i-th atom, η_i is the corresponding phase term, r_{ij} is the internuclear separation between atoms i and j, l_{ij} is the corresponding mean amplitude of vibration, and C is a proportionality constant. A proper Fourier analysis can highlight the modulation in $\sin(sr_{ij})/sr_{ij}$ term, resolving the structure information of molecules. One advantage of diffraction method implied in Eq. (6) is that it contains structure information from all atom–atom pairs, unlike the spectroscopy where only specific transitions can be monitored.[15] So, there is a great hope that by adding temporal resolution, gas-phase UED can resolve the structures of molecules in short-lived excited states or finding intermediate products in a chemical reaction. Starting from millisecond, the temporal resolution of gas-phase UED reaches ps range in 1990s, and now is improved to around 100 fs. This allows the study of dissociation reaction of $C_2F_4I_2$,[42,43] dark structures in molecular radiationless transitions,[44] and many more.[15,45]

One challenge for gas-phase UED is the very weak signal from molecules. In a pump–probe experiment, only a small portion of molecules (less than 10%) are excited such that the the small change in $I_{\rm M}$ is buried by the unchanged background. Even if all the molecules are excited, it is well-known that $I_{\rm M}$ is at least one order smaller than $I_{\rm A}$ which contains no structure information. The high electron fluence provided by our new instrument is expected to boost the research activities in this area.

4.2. Coupling among multiple degrees of freedom and associated lattice dynamics

Structural dynamics is correlated to electrons, spins, and other degrees of freedom. Understanding the nature of coupling among them is crucial in understanding the properties of materials. Selectively perturbing one degree of freedom and monitoring the subsequent response from others proves to be an effective way in separating various coupling processes.

As one example, ultrafast laser heating is used to trigger both electron and lattice dynamics. In this case, electrons first absorb photon energy and are pumped to exited states. Their subsequent relaxation process has been studied by various methods. Particularly, by electron–phonon coupling, electrons transfer energy to lattice which induces an increase of lattice temperature (lattice heating) and lattice expansion. According to Eq. (1), any change in lattice constants results in a change in diffraction angles following $\Delta\theta/\theta \approx -\Delta d_{(h,k,l)}/d_{(h,k,l)}$ by which lattice expansion can be monitored. Benefiting from the long range orders in lattice, now UED can resolve a lattice constant change as tiny as 0.01%.[46] Meanwhile, lattice heating would decrease the intensity of diffraction peaks following

the Debye–Waller relation

$$I_{h,k,l} \propto \exp\left(\frac{-B(T)(h^2+l^2+k^2)}{2a^2}\right), \quad (7)$$

where $I_{h,k,l}$ represents the overall intensity of the diffraction peak specified by Miller indices (h,k,l). $B(T)$ is the Debye–Waller factor that increases linearly with increasing temperature to the first order approximation.

In a conventional static measurement, it seems that lattice heating and lattice expansion happen concurrently very much like one process. Now by using UED, these two process can be monitored simultaneously and clearly separated in time domain as two different aspects of lattice dynamics. The time constant for lattice heating is measured for various metals[47,48] and semiconductors,[49–53] ranging from several hundred fs to several ps. On the other hand, the timescale of lattice expansion is not only determined by the driving force but also the boundary conditions. Accompanied by thermal expansion, lattice coherent motion can also be generated as optical phonon modes[54] or acoustic phonon modes.[55,56] It is worth mentioning that lattice heating in ultrafast time-scale can be phonon-momentum dependent, i.e., certain phonon modes couple more strongly to electrons, and they are initially populated before a universal lattice temperature is established. This can be investigated by analyzing the diffused scattering background between Bragg peaks, which provides more insights in the transient lattice dynamics.[57–59]

Pumping with even higher laser fluence, the long range orders in lattice finally break and melting occurs, which is the most common structure phase transition in nature yet a sound link between macroscopic phenomena and atomic-level dynamics is still lacking.[5] As a priority, melting has been investigated extensively by UED.[5,60] It is shown that melting is purely thermal-driven in aluminum,[17] while in gold, a surprising phonon harding effect (slow down in melting) due to weakened screening from electrons has been observed under high laser fluence.[61] The effect from electron system on lattice melting is even more profound in semiconductor silicon[62] and Peierls distorted system bismuth.[63] Accompanied by lattice melting, the state of warm dense matter is reached under certain conditions[64] when the potential energy and the kinetic energy of electrons are of roughly the same magnitude. This is a new frontier of physics, where UED can provide insights of the related lattice dynamics[65] and together with the evolution of the spatial distribution.[66]

Melting is one example of an irreversible process, in which samples cannot recover to their original condition after each excitation cycle. So UED must provide enough electron fluence to construct a diffraction pattern with just one shot for each time point on the transient curve. Now with our new apparatus that can bunch up to one million electrons, more materials can be studied with even finer structure details by such single-shot experiment. There are also reversible structure phase transitions where stroboscopical mode can be applied. During these processes, certain characteristic Bragg spots will appear or disappear reflecting the symmetry change of the lattice. As examples, the transient lattice dynamics of strong correlated systems such as lanthanum strontium manganite (LSMO),[67] vanadium dioxide (VO_2),[68,69] and quasi-two-dimension dichalcogenide [70–74] are studied.

4.3. Surface science and beyond

RHEED and LEED are powerful tools of structure characterization and surface science, and there have been great effort to develop time-resolved RHEED (TR-RHEED) and LEED (TR-LEED). Although the beam energy of LEED is as low as 20 eV very different from RHEED, so far they use similar strategies to reduce space-charge effect and gain temporal resolution. TR-RHEED develops vary rapidly whose temporal resolution was improved from initially 200 ps to sub-ps,[50,75] while TR-LEED is still in its infancy.[76,77] By using TR-RHEED, surface lattice dynamics is investigated for GaAs and its quantum well,[50] sillicon,[78] graphite,[79] bismuth,[80] surface water,[81] cuprate,[82] and so on. One advantage of TR-RHEED is the use of bulk material which largely simplifies the sample preparation, but it also makes diffraction signal weak due to only nm penetration depth of electrons at such a small glancing angle (see Fig. 2(b)). Benefiting from the pulse compression scheme, now the signal to noise ratio in such study can be significantly improved. Meanwhile, the energy of electrons is still in the keV range, not too high for the glancing angle to be resolved. Another issue for TR-RHEED is the transient charging induced by pump that can deflect the electron probe.[7–9] Such effect must be carefully suppressed by choosing proper pump fluence and photon wavelength, or eliminated from signal by theoretical modeling. Turning disadvantage into opportunities, ultrafast electrons have been used to monitor the transient electric field distribution of various materials beyond TR-RHEED application.[8,83] Attaching molecules, nanoparticles,[84] or low dimension structures on a surface [85] create new opportunities to study catalysis, functional materials, and sample-substrate correlations by UED, yet this field is still waiting for further exploration.

5. Conclusion and perspectives

Directly monitoring lattice dynamics to understand the structure-function correlations is a very important goal for ultrafast science. Previously, such information is usually obtained by various optical methods such as ultrafast x-ray diffraction, ultrafast Raman spectroscopy, and so on. Electron-probe based techniques such as UED and UEM are entering

this field, offering atomic-level temporal and spacial sensitivities with only lab-scale instrumentation. Now, new methodologies and techniques are emerging that hold great promise to push UED's temporal resolution to sub-fs scale, use all-optical method to manipulate the electron bunch in 3D, and generate high coherent electrons by ultra-cold sources. Together with a synergic use of other ultrafast techniques, UED will give a big impact on dynamical studies in various areas in the future.

References

[1] Kabius B C, Browning N D, Thevuthasan S, Diehl B L and Stach E A 2012 *Dynamic processes in biology chemistry and materials science: Opportunities for ultrafast transmission electron microscopy-workshop summary report Technical report Pacific Northwest National Laboratory (PNNL)*, Richland, WA (US)

[2] Williams D B 2009 *Transmission Electron Microscopy — a Textbook for Materials Science*

[3] Thomas J M and Midgley P A 2011 *Chem. Phys.* **385** 1

[4] King W E, Armstrong M, Campbell G, Frank A, Reed B and Stuart B 2005 *J. Appl. Phys.* **97** 8

[5] Sciaini G and Miller R J D 2011 *Rep. Prog. Phys.* **74** 96101

[6] Henderson R 1995 *Q. Rev. Biophys.* **28** 171

[7] Park H and Zuo J M 2009 *Appl. Phys. Lett.* **94** 587

[8] Raman R K, Tao Z S, Han T R and Ruan C Y 2009 *Appl. Phys. Lett.* **95** 024912

[9] Schfer S, Liang W and Zewail A H 2010 *Chem. Phys. Lett.* **493** 11

[10] Qian B L and Elsayedali H E 2002 *J. Appl. Phys.* **91** 462

[11] Li M C, Wang X, Liao G Q, Li Y T and Zhang J 2017 *Chin. Phys. B* **26** 054103

[12] Reed B W 2006 *J. Appl. Phys.* **100** 44

[13] Siwick B J, Dwyer J R, Jordan R E and Miller R J D 2002 *J. Appl. Phys.* **92** 1643

[14] Michalik A M, Ya E and Sipe J E 2008 *J. Appl. Phys.* **104** 054905

[15] Srinivasan R, Lobastov V A, Ruan C Y and Zewail A H 2003 *Cheminform* **34** 1761

[16] Cao J, Hao Z, Park H and Tao C 2003 *Appl. Phys. Lett.* **83** 1044

[17] Siwick B J, Dwyer J R, Jordan R E and Miller R J 2003 *Science* **302** 1382

[18] Waldecker L, Bertoni R and Ernstorfer R 2015 *J. Appl. Phys.* **117** 1382

[19] Badali D S, Gengler R Y N and Miller R J D 2016 *Structural Dyn.* **3** 034302

[20] Yurtsever A and Zewail A H 2009 *Science* **326** 708

[21] Zewail A H and Thomas J M 2009 *4D Electron Microscopy: Imaging in Space and Time* (Imperial College Press)

[22] Cao G L, Sun S S, Li Z W, Tian H F, Yang H X and Li J Q 2014 *Sci. Rep.* **5** 8404

[23] Eichberger M, Erasmus N, Haupt K, Kassier G, Von Flotow A, Demsar J and Schwoerer H 2013 *Appl. Phys. Lett.* **102** 1382

[24] Li R, Tang C, Du Y, Huang W, Du Q, Shi J, Yan L and Wang X 2009 *Rev. Sci. Instrum.* **80** 083303

[25] Hastings J, Rudakov F, Dowell D, Schmerge J, Gierman S and Weber P 2006 *Appl. Phys. Lett.* **89** 161

[26] Zhu P, Berger H, Cao J, Geck J, Hidaka Y, Kraus R, Pjerov S, Shen Y, Tobey R I and Zhu Y 2016 *New J. Phys.* **17** 063004

[27] Zhu P F, Fu F C, Liu S G, Xiang D, Zhang J and Cao J M 2014 *Chin. Phys. Lett.* **31** 116101

[28] Musumeci P, Moody J T, Scoby C M, Gutierrez M S and Westfall M 2010 *Appl. Phys. Lett.* **97** 65

[29] Murooka Y, Naruse N, Sakakihara S, Ishimaru M, Yang J and Tanimura K 2011 *Appl. Phys. Lett.* **98** 285

[30] Weathersby S P, Brown G, Centurion M, Chase T F, Coffee R, Corbett J, Eichner J P, Frisch J C, Fry A R and Ghr M 2015 *Rev. Sci. Instrum.* **86** 28

[31] Yang J, Koichi K, Kondoh T, Yoshida Y, Tanimura K and Urakawa J 2014 *Nucl. Inst. & Methods Phys. Res. A* **637** S24

[32] van Oudheusden T, Pasmans P L E M, van der Geer S B, de Loos M J, van der Wiel M J and Luiten O J 2010 *Phys. Rev. Lett.* **105** 264801

[33] Chatelain R P, Morrison V R, Godbout C and Siwick B J 2012 *Appl. Phys. Lett.* **101** 73

[34] Qi Y P, Pei M J, Qi D L, Li J, Yang Y, Jia T, Zhang S and Sun Z R 2017 *New J. Phys.* **19** 023015

[35] Baum P 2014 *J. Phys. B At. Mol. & Opt. Phys.* **47** 124005

[36] Altucci C, Velotta R and Marangos J P 2010 *J. Mod. Opt.* **57** 916

[37] Morimoto Y and Baum P 2017 *Nature Physics* **14** 252

[38] Zhang P, Yang J and Centurion M 2014 *New J. Phys.* **16** 083008

[39] Baum P and Zewail A H 2006 *Proc. Natl. Academy Sci. United States Am.* **103** 16105

[40] van Mourik M W, Engelen W J, Vredenbregt E J D and Luiten O J 2014 *Structural Dyn.* **1** 034302

[41] Hoffrogge J, Paul Stein J, Kruger M, Forster M, Hammer J, Ehberger D, Baum P and Hommelhoff P 2014 *J. Appl. Phys.* **115** 65

[42] Ihee H, Lobastov V A, Gomez U M, Goodson B M, Srinivasan R, Ruan C Y and Zewail A H 2001 *Science* **291** 458

[43] Reckenthaeler P, Centurion M, Fuss W, Trushin S A, Krausz F and Fill E E 2009 *Phys. Rev. Lett.* **102** 213001

[44] Srinivasan R, Feenstra J S, Park S T, Xu S and Zewail A H 2005 *Science* **307** 558

[45] Centurion M 2016 *J. Phys. B* **49** 062002

[46] Park H, Wang X, Nie S, Clinite R and Cao J 2005 *Phys. Rev. B* **72** 301

[47] Wang X, Nie S, Li J, Clinite R, Clark J E and Cao J 2010 *Magn. Phys. Rev. B* **81** 220301

[48] Nie S, Wang X, Park H, Clinite R and Cao J 2006 *Phys. Rev. Lett.* **96** 025901

[49] Harb M, Ernstorfer R, Dartigalongue T, Hebeisen C T, Jordan R E and Miller R J D 2006 *J. Phys. Chem. B* **110** 25308

[50] Yang D S, Gedik N and Zewail A H 2007 *J. Phys. Chem. C* **111** 4889

[51] Wang X, Rahmani H, Zhou J, Gorfien M, Plaskus J M, Li D, Voss R, Nelson C A, Lei K W and Wolcott A 2016 *Appl. Phys. Lett.* **109** 773

[52] Schfer S, Liang W and Zewail A H 2011 *New J. Phys.* **13** 063030

[53] Schfer S, Liang W and Zewail A H 2011 *Chem. Phys. Lett.* **515** 278

[54] Chatelain R P, Morrison V R, Klarenaar B L and Siwick B J 2014 *Phys. Rev. Lett.* **113** 235502

[55] Harb M, Peng W, Sciaini G, Hebeisen C T, Ernstorfer R, Eriksson M A, Lagally M G, Kruglik S G and Miller R J D 2009 *Phys. Rev. B* **79** 4301

[56] Park H, Nie S, Wang X, Clinite R and Cao J 2005 *J. Phys. Chem. B* **109** 13854

[57] Chase T, Trigo M, Reid A H, Li R, Vecchione T, Shen X, Weathersby S, Coffee R, Hartmann N and Reis D A 2016 *Appl. Phys. Lett.* **108** 1175

[58] Waldecker L, Bertoni R, Vorberger J and Ernstorfer R 2015 *Phys. Rev. X* **6** 021003

[59] Waldecker L, Bertoni R, Hbener H, Brumme T, Vasileiadis T, Zahn D, Rubio A and Ernstorfer R 2017 *Phys. Rev. Lett.* **119** 036803

[60] Williamson S, Mourou G and Li J C M 1984 *Phys. Rev. Lett.* **52** 2364

[61] Ernstorfer R, Harb M, Hebeisen C T, Sciaini G, Dartigalongue T and Miller R J D 2009 *Science* **323** 1033

[62] Harb M, Ernstorfer R, Hebeisen C T, Sciaini G, Peng W, Dartigalongue T, Eriksson M A, Lagally M G, Kruglik S G and Miller R J D 2008 *Phys. Rev. Lett.* **100** 155504

[63] Sciaini G, Harb M, Kruglik S G, Payer T, Hebeisen C T, Heringdorf Fj Zu, Yamaguchi M, Hornvon M, Ernstorfer R and Miller R J D 2009 *Nature* **458** 56

[64] Koenig M, Benuzzimounaix A, Ravasio A, Vinci T, Ozaki N, Lepape S, Batani D, Huser G, Hall T and Hicks D 2005 *Plasma Phys. & Control. Fusion* **47** 481

[65] MoMZ, Shen X, Chen Z, Li R K, Dunning M, Sokolowskitinten K, Zheng Q, Weathersby S P, Reid A H and Coffee R 2016 *Rev. Sci. Instrum.* **87** 11D810

[66] Li J, Zhou J, Ogitsu T, Ping Y, Ware D and Cao J 2012 *High Energy Density Phys.* **8** 298

[67] Li J, Wang X, Zhou H, Zhou J, Cheng J G and Cao J 2016 *Appl. Phys. Lett.* **109** 337

[68] Morrison V R, Chatelain R P, Tiwari K L, Hendaoui A, Bruhcs A, Chaker M and Siwick B J 2014 *Science* **346** 445

[69] Tao Z, Zhou F, Han T R T, Torres D, Wang T, Sepulveda N, Chang K, Young M, Lunt R R and Ruan C Y 2016 *Nat. Sci. Rep.* **6** 38514

[70] Sun S, Wei L, Li Z, Cao G, Liu Y, Lu W J, Sun Y P, Tian H, Yang H and Li J 2015 *Phys. Rev. B* **92** 224303

[71] Wei L, Sun S, Cong G, Li Z, Kai S, Yu L, Lu W, Sun Y, Tian H and Yang H 2017 *Structural Dynamics* **4** 044012

[72] Han T R T, Zhou F, Malliakas C D, Duxbury P M, Mahanti S D, Kanatzidis M G and Ruan C Y 2015 *Sci. Adv.* **1** e1400173

[73] Le G L, Chase T, Reid A H, Li R K, Svetin D, Shen X, Vecchione T, Wang X J, Mihailovic D and Drr H A 2017 *Structural Dynamics* **4** 044020

[74] Erasmus N, Eichberger M, Haupt K, Boshoff I, Kassier G, Birmurske R, Berger H, Demsar J and Schwoerer H 2012 *Phys. Rev. Lett.* **109** 3076

[75] ElsayedAli H E and Herman J W 1990 *Rev. Sci. Instrum.* **61** 1636

[76] Vogelgesang S, Storeck G, Horstmann J G, Diekmann T, Sivis M, Schramm S, Rossnagel K, Schfer S and Ropers C 2017 *Nature Physics* **14** 184

[77] Gulde M, Schweda S, Storeck G, Maiti M, Yu H K, Wodtke A M, Schfer S and Ropers C 2014 *Science* **345** 200

[78] Hassan M T 2018 *J. Phys. B* **51** 032005

[79] Raman R K, Murooka Y, Ruan C Y, Yang T, Berber S and Tomnek D 2008 *Phys. Rev. Lett.* **101** 077401

[80] Krenzer B, Hanisch-Blicharski A, Schneider P, Payer T, M?Llenbeck S, Osmani O, Kammler M, Meyer R and Hoegen H V 2009 *Phys. Rev. B* **80** 1132

[81] Ruan C Y, Lobastov V A, Vigliotti F, Chen S and Zewail A H 2004 *Science* **304** 80

[82] Gedik N, Yang D S, Logvenov G, Bozovic I and Zewail A H 2007 *Science* **316** 425

[83] Long C, Li R, Chen J, Zhu P, Liu F, Cao J, Sheng Z and Zhang J 2015 *Proc. Natl. Academy Sci. United States Am.* **112** 14479

[84] Frigge T, Hafke B, Tinnemann V, Witte T and Hoegen H V 2015 *Structural Dynamics* **2** 035101

[85] Frigge T, Hafke B, Witte T, Krenzer B, Streubhr C, Syed A S, Trontl V M, Avigo I, Zhou P and Ligges M 2017 *Nature* **544** 207